CrossMark

ORIGINAL ARTICLE

# Organocatalytic Fluorogenic Synthesis of Chromenes

Mina Raeisolsadati Oskouei[1] · Albert M. Brouwer[1]

**Abstract** Two fluorescent derivatives of 2-amino-3-carbonitrile-4H-chromene were synthesized by means of a fluorogenic Michael addition of dimedone to dicyano alkene labeled BODIPY derivatives. Different organocatalysts were used in different conditions to obtain compounds 3 and 4 in good yield (up to 65% and 85%) and moderate enantiomeric excess (51% and 41% ee, respectively). This work provides the first example of an enantioselective organocatalytic conversion combined with fluorogenesis.

**Keywords** Chromene · Fluorescence spectroscopy · Organocatalysis · Fluorogenic reaction

## Introduction

Chemical reactions that generate a bright fluorescent species are called "fluorogenic". Such fluorescence turn-on is often used as a way to construct fluorescent markers for a particular substrate based on a reaction between the marker and a fluorophore precursor [1–6]. In our laboratory we have initiated a research program aimed at the study of organocatalytic reactions using fluorescence spectroscopy [7–9]. In this connection we explore fluorogenic reactions as a first step towards unravelling the details of the reaction mechanisms [10–12]. The present paper describes a novel fluorogenic organocatalytic reaction in which a fluorescent chromene derivative 3 is produced from the almost non-fluorescent precursor 1 [6, 13].

Chromene is a structural component in biologically active and natural compounds such as alkaloids, tocopherols, flavonoids, and anthocyanins [14–17]. Functionalized chromenes have attracted a lot of attention in the field of synthetic and medicinal chemistry [18–23]. Among the diverse chromene derivatives, 2-amino-4H-chromenes are reported as potential drugs in the treatment of human inflammatory TNFa-mediated diseases [24]. Cytotoxicity of 2-amino-3-carbonitrile-4H-chromene in human acute myeloid leukemia (AML) cell lines has been demonstrated. These compounds bind to the surface pocket of the cancer-implicated Bcl-2 protein and induce apoptosis or programmed cell death in follicular lymphoma B cells and leukemia HL-60 cells [25–27]. Luminescent labeling of cells is used for flow cytometry and microscopy [28–30]. The function of the cells can, however, be affected by the dye. Furthermore, some dyes cannot be used in combination with other dyes [31]. Having a broader spectrum of dyes provides more possibilities for researchers to overcome the limitations of the available ones. Especially, if the labeling agent is the drug itself, it will be possible to detect the components of the biological assemblies and imaging and flow cytometry at the same time. In this case, there is hope to find the mechanism of the interaction between the drug and the tumor cell to design more effective drugs. Thus, although it is not the primary aim of our study, the dye-labelled chromenes may find applications in biomedical research.

BODIPY (4,4-difluoro-4-bora-3a,4a-diaza-s-indacene) dyes are often the preferred choice for labelling applications. They are relatively nonpolar and the chromophore is electrically neutral. These properties tend to minimize dye-induced perturbation of the functionality of the labelled species [32–35].

✉ Albert M. Brouwer
A.M.Brouwer@uva.nl

[1] van 't Hoff Institute for Molecular Sciences, University of Amsterdam, PO Box 94157, 1090 GD Amsterdam, The Netherlands
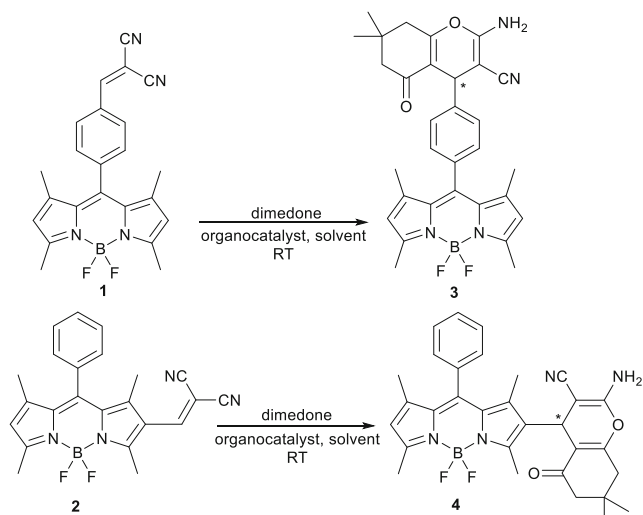
**Scheme 1** Synthesis of 2-amino-3-carbonitrile-4H-chromenes **3** and **4**

In the present work we couple two dicyano alkene derivatives of BODIPY (compounds **1** and **2**) [6, 13, 36–38], with dimedone to produce the corresponding fluorescent chromenes (Scheme 1). Compounds **1** and **2** have been used as a fluorescent turn-on and turn-off probes, respeectively, for the detection of cyanide in solution [37, 38]. To the best of our knowledge there is no report about the application of compounds **1** and **2** in organocatalytic synthetic reactions. In this article we present the main results of the first usage of these compound in organocatalytic Michael addition reactions, which are followed up in situ by a ring closure leading to chromenes.

In compounds **1** and **2** the BODIPY skeleton is responsible for the fluorescence. In compound **1** the fluorescence is strongly quenched by a photo induced electron transfer mechanism [37]. The BODIPY part of the molecule acts as an electron donor [39, 40], the dicyanoalkene as the electron acceptor. In this compound the two units are not effectively conjugated because the 8-phenyl substituent is almost orthogonal to the BODIPY [40]. In compound **2**, on the other hand, the fluorescence is not quenched. In this case, the dicyanoalkene group is directly conjugated with the BODIPY unit, and the excited state has mostly a delocalized π-π* character [36].

The Michael addition to the double bond of the dicyano alkene in **1** turns on the fluorescence because this effectively removes the electron acceptor unit. This phenomenon allows us to use fluorescence spectroscopy to follow the addition of the nucleophile, deprotonated dimedone in this case, to form compound **3** after a ring closure step.
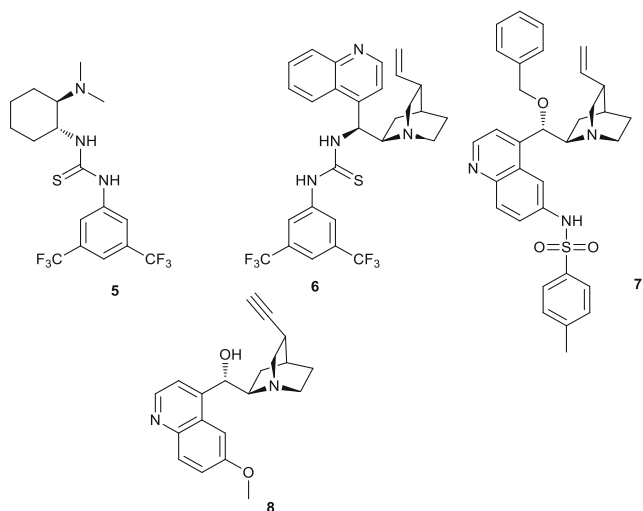
The ability of hydrogen bond forming catalysts to speed up and control the enantioselectivity of the Michael addition reactions has been amply demonstrated. Among the many available catalysts, we selected catalysts **5–8** which have been reported to promote Michael additions in high yield and enantioselectivity (Scheme 2) [41, 42].

In these catalysts, the amine group provides the required basicity to produce the nucleophilic dimedone anion and the hydrogen bond donating groups can activate the Michael acceptor by hydrogen bonding to the cyano groups.

## Results and Discussion

The reaction between dicyanoalkene-BODIPY **1** and dimedone was performed using different catalysts in dichloromethane (DCM) at room temperature (Table 1).

The enantioselectivity in the presence of catalyst **6** is similar to that obtained with catalyst **5** and is low in the presence of catalysts **7** and **8**. The result of the reactions between dicyanoalkene-BODIPY **1** and dimedone in the presence of catalyst **5** showed catalysis of the reaction in both polar and non-polar solvents at room temperature (Table 2). Reaction in DCM and toluene at room temperature provided the product

**Table 1** Reaction between dimedone and compound **1** in the presence of different catalysts in DCM at room temperature

| Catalyst (10 mol%) | 5 | 6 | 7 | 8 |
|---|---|---|---|---|
| ee (%) | 44 | 42 | 20 | 10 |
| Yield (%) | 80 | 85 | 73 | 70 |



**Scheme 2** Organocatalysts used

**Table 2** Reaction between dimedone and compound **1** in the presence of catalyst **5** (10 mol%)

| Solvent | Toluene | DCM | DCM | DCM | THF |
|---|---|---|---|---|---|
| Temperature (°C) | 25 | 25 | 0 | -20 | 25 |
| ee (%) | 42 | 44 | 44 | 51 | 0 |

**Table 3** Reaction between dimedone and compound **2** in the presence of different catalysts at room temperature

| Catalyst (10 mol%) | 5 | 5 | 6 | 7 | 8 |
|---|---|---|---|---|---|
| Solvent | Toluene | DCM | DCM | DCM | DCM |
| ee (%) | 27 | 34 | 41 | 12 | 34 |
| Yield (%) | 65 | 68 | 72 | 68 | 65 |

with 42–44% enantiomeric excess (ee). The reaction in tetrahydrofuran (THF) was not enantioselective. The progress of the reaction was followed in DCM at different temperatures (Table 2). Decreasing the temperature slows down the reaction, but the enantiomeric excess is higher.

We applied similar conditions for the reactions between compound **2** and dimedone in the presence of the different catalysts (Table 3).

In compound **2** conjugation of the double bond of the dicyano alkene group with the pyrrole moiety of the BODIPY decreases the nucleophilicity of this group. As a result, the reaction with dimedone is slower for compound **2** than for compound **1**. The structural assignments are provided in the Supporting Information.
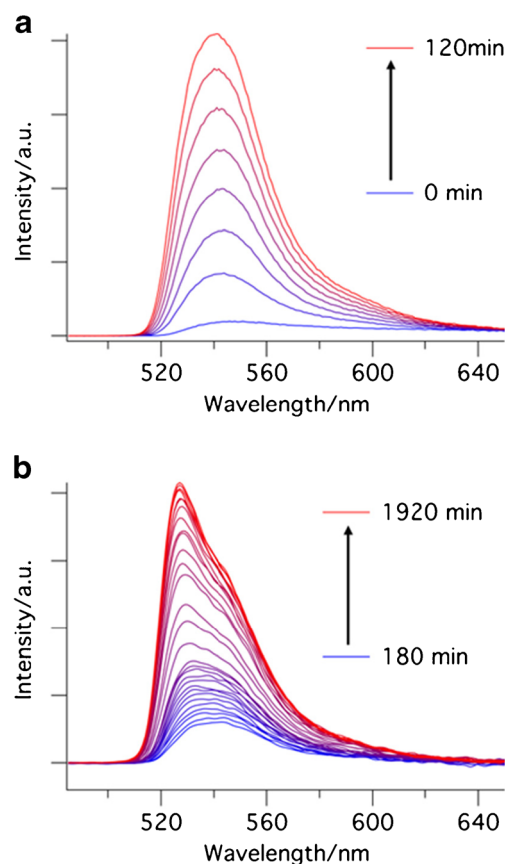
We determined photophysical properties of the pure reactants and products by means of absorption and fluorescence spectroscopy, and time-resolved fluorescence [43–45]. The results are summarized in Table 4. The absorption spectra are all similar, as expected, with small red shifts for **2** and **4**, in which the BODIPY core is substituted. The absorption coefficients and radiative rate constants are similar, and characteristic for the BODIPY chromophore.

The fluorescence decays of compounds **2**, **3**, and **4** are described very well by a mono-exponential model. In the case of compound **1**, however, we observed a tri-exponentially decaying intensity with a time constant of ~10 ps for the major fraction, corresponding to the strongly quenched fluorescence. The time resolution of our set-up is insufficient to resolve this properly, so the real time constant may be smaller than 10 ps. A slow decay component is present with a time constant similar to that of the other BODIPY derivatives and may be due to a minor impurity in the sample. A third component with an



**Fig. 1** Emission spectra ($\lambda_{ex}$ = 478 nm) of the mixture of the reaction between dimedone and compound 1 in the presence of catalyst **5** in DCE at room temperature. **a** during the first two hours, **b** during the later stages of the reaction

intermediate decay time is clearly present, however. Further research will be needed to ascertain its origin.

We applied fluorescence spectroscopy to follow the progress of the Michael reaction. In order to be able to measure the fluorescence of the reaction mixture directly, an HPLC pump was used to circulate the solution through a microcuvette in the sample compartment of the fluorescence spectrometer. Because the optical path length is short, internal filter effects are less important. By using the circulation pump we can work with practically manageable quantities of material and a reaction volume of 4 mL, and provide for continuous mixing of the reagents.

**Table 4** Photophysical parameters of compounds **1**, **2**, **3** and **4** in DCM

| Compound | $\lambda_{max, abs}$[a] (nm) | $\varepsilon$[b] ($10^3$ L mol$^{-1}$ cm$^{-1}$) | $\lambda_{em}$[c] (nm) | $\phi_f$[d] | $\tau$[e] (ns) | $k_f$[f] (s$^{-1}$) | $k_{nr}$[g] (s$^{-1}$) |
|---|---|---|---|---|---|---|---|
| 1 | 505 | 75 | 517 | 0.025 | 0.01(0.57); 1.4 (0.30); 3.1 (0.13) | | |
| 2[h] | 516 (514) | 77 (55) | 532 (543) | 0.54 (0.45) | 3.08 | $1.7 \times 10^8$ | $1.5 \times 10^8$ |
| 3 | 500 | 74 | 511 | 0.45 | 3.50 | $1.3 \times 10^8$ | $1.6 \times 10^8$ |
| 4 | 512 | 78 | 523 | 0.61 | 3.94 | $1.6 \times 10^8$ | $1.0 \times 10^8$ |

[a] Absorbance maximum, [b] Molar absorption coefficient, [c] Emission maximum, [d] Quantum yield, [e] Decay time; for **1** the three time constants are given with amplitudes in parentheses, [f] Fluorescence rate constant $k_f = \phi_f/\tau$, [g] Non-radiative rate constant $k_{nr} = \tau^{-1} - k_f$, [h] Literature values from ref. 11c are given in parentheses

**Scheme 3** Mechanism of formation of compound **3**



**Fig. 3** Emission spectra of compound **2** in dichloromethane at different concentrations ($\lambda_{ex}$ = 478 nm)

The emission spectrum of the mixture was measured every 30 min for 32 h. In order to decrease the error due to evaporation of the solvent and changing the concentration of the mixture, we used the less volatile dichloroethane (DCE) as the solvent instead of DCM. The emission of the solution of compound **1** in DCE was measured. Then, catalyst **5** and dimedone were added to the solution. The increase of the intensity of fluorescence, already clearly visible after 5 min, shows formation of the product. This increase slows down after 25 h (Fig. 1).

It is evident that the shape of the spectrum changes during the course of the reaction. Initially, the product spectrum is broad and peaks at ~540 nm (Fig. 1(a)), later it shows a pronounced peak at 532 nm (Fig. 1(b)). We tentatively attribute this change to the presence of a distinct intermediate, which initially builds up, and then decays as the final product is formed in a cyclization reaction (See Scheme 3).

In contrast to compound **1** [6, 13, 37], its isomer **2** is strongly fluorescent [36, 38]. The direct interaction of the dicyano alkene group with the pyrrole moiety increases the length of the conjugated system, which leads to red shifted absorption and emission spectra, but also to lower reactivity because the electron rich BODIPY donates some electron density to the Michael acceptor group. As a result, the reaction of compound **2** with dimedone is clearly slower (Fig. 2) than that of **1**.

We note that the shape and the position of the emission spectrum of compound **2** and its reaction product in this

experiment are notably different from the spectra at low concentrations that were used to determine the photophysical properties. The red-shifted and broadened spectra are due to the higher concentrations used in the reaction mixture. At higher concentrations the second shoulder appears at longer wavelengths. The intensity of this new shoulder increases by increasing the concentration. This change can arise from aggregation of the chromphores (Fig. 3). During the reaction leading to product 4, we observe only a small change in the intensity of the emitted light and no change of the spectral shape.

## Conclusion

This work provides a simple method to synthesize labeled chromenes with good yields and enantiomeric excess, and introduces fluorescence spectroscopy as a powerful tool to follow the reaction of the fluorogenic substrate **1**. An intermediate of the two-step reaction could be detected by its fluorescence spectrum that is different from that of the product. The fluorescence of products **3** and **4** allows these compounds to be screened using imaging methods and opens a new avenue for the study of the efficiency of these compounds in the treatment of diseases.

## Experimental

### Materials and Methods

All commercially available reagents and solvents were used as received. Catalyst **5** was obtained from Sigma Aldrich. Catalysts **6** and **8** were synthesized following the literatures procedures [46, 47]. Catalyst **7** was prepared in the organic synthesis group of the University of Amsterdam [48]. Flash column chromatography was carried out using silica gel 60A, 0.040–0.063 mm. Commercially available pre-coated TLC plastic sheets (Silica gel 60 F254) were used for thin layer
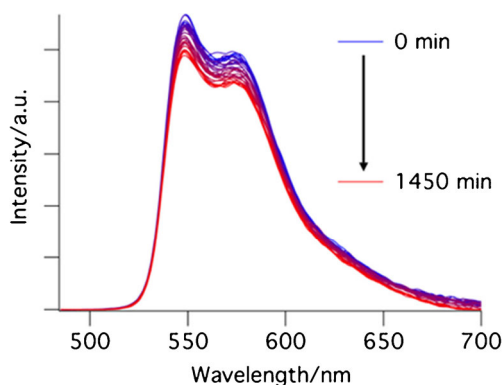


**Fig. 2** Emission spectra of the mixture of the reaction between dimedone and compound **2** in the presence of catalyst **5** in DCE at room temperature ($\lambda_{ex}$ = 478 nm)
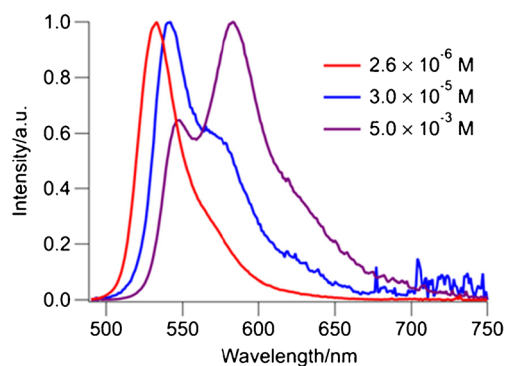
chromatography (TLC). Preparative TLC was carried on commercially available pre-coated TLC glass plates (PLC Silica gel 60 F254, 1 mm). A UV lamp (254 or 366 nm) was used for visualization. Chiral HPLC was performed using a Shimadzu LC-20 AD liquid chromatograph equipped with SPD-M20A diode array detector and chiral OD-H column. 20% Isopropanol in heptane was used as the eluent. 1H and 13C NMR spectra were recorded on a Bruker Avance 400 spectrometer and analyzed using the MestReNova v 7.1.2 (Mestrelab Research S.L.) software. Signal positions were recorded in $\delta$ ppm with the abbreviations s, d, dd and m denoting singlet, doublet, doublet of doublets and multiplet respectively. All 1H NMR chemical shifts are referenced to $SiMe_4$ as an external standard (0.00 ppm). All 13C NMR chemical shifts in $CDCl_3$ were referenced to the residual solvent peak at 77.00 ppm but are reported vs. tetramethylsilane. All coupling constants, J, are quoted in Hz. Infra-red spectra were recorded on a Bruker IR spectrometer model $\alpha$-Platinum ATR using neat solid samples. Mass spectra were collected on an AccuTOF LC, JMS-T100LP Mass spectrometer (JEOL, Japan). The measurement conditions were as follows: Positive-ion mode; Needle voltage 2000 V, Orifice 1 voltage 90 V, Orifice 2 voltage 9 V, Ring Lens voltage 22 V. Ion source temperature 30 °C, spray temperature − 20 °C. Flow injection with a flow rate of 0.01 ml/min. The UV-Vis absorption spectra were recorded on a double beam Shimadzu UV-2700 spectrophotometer. Fluorescence excitation and emission spectra of the compounds were recorded using a SPEX Fluorolog 3–22 fluorimeter. The concentrations were chosen to have A = 0.1 in a 1 cm cell at the excitation wavelength (c $\approx$ $10^{-6}$ M). A Gilden Photonics FluoroSense-M series spectrometer equipped with two double monochromators was used to follow the reactions. A Bischoff HPLC pump was used to circulate the solution. DCM dye (4-(dicyanomethylene)-2-methyl-6-(4-dimethylaminostyryl)-4H–pyran) was used as the reference to determine the fluorescence quantum yields ($_f$ = 0.43) [49]. The measurement of fluorescence decay times was performed as described in reference [9]. The excitation wavelength was $\lambda_{ex}$ = 478 nm. Decay curves were fitted to a sum of exponential decays using a nonlinear least-squares routine implemented in Igor Pro 6.3 (Wavemetrics, Inc.). In all cases the $\chi^2$ value was <1.1, indicating excellent fits.

## Synthesis of 1

Compound **1** (8-(4-(2,2-dicyanovinyl)phenyl)-4,4-difluoro-1,3,5,7-tetramethyl-4-bora-3a,4a–diaza-s-indacene) was prepared according to references [6, 13]. Analytical data are in agreement with the literature.

## Synthesis of 2

Compound **2** (6-(2,2-dicyanovinyl)-8-phenyl-4,4-difluoro-1,3,5,7-tetramethyl-4-bora-3a,4a-diaza-s-indacene) was prepared according to reference [37]. Analytical data are in agreement with the literature.

## Synthesis of 3

Compound **1** (40 mg, 0.1 mmol) was dissolved in 4 ml solvent (see Table 2), dimedone (15.4 mg, 0.11 mmol) and organocatalysts (0.01 mmol) were added. The mixture was stirred at room temperature for 24 h. The product was purified using flash column chromatography (25% EtOAc/petroleum ether). 1H NMR (400 MHz, $CDCl_3$): $\delta$ (ppm) = 7.43 (d, 2H, J = 8 Hz, ArH), 7.23 (d, 2H, J = 8 Hz, ArH), 5.98 (s, 2H, CH-pyrrole), 4.61 (s, 2H, $NH_2$), 4.52 (s, 1H, CH), 2.56 (s, 6H, $CH_3$), 2.48 (AB pattern, 2H, $\Delta\delta AB$ = 0.09 ppm, J = 20 Hz, $CH_2$), 2.23 (AB pattern, 2H, $\Delta\delta AB$ =0.16 ppm, J = 16 Hz, $CH_2$), 1.35 (s, 6H, $CH_3$), 1.14 (s, 3H, $CH_3$), 0.98 (s, 3H, $CH_3$). 13C NMR (100 MHz, $CDCl_3$): 195.24, 161.11, 157.46, 154.18, 144.04, 143.09, 133.59, 128.52, 127.87, 121.02, 117.99, 113.85, 99.81, 62.89, 50.45, 40.48, 35.35, 31.92, 28.97, 26.72, 14.39, 14.09. IR: $\nu$ ($cm^{-1}$): 3450, 3338, 3220, 2954, 2192, 1676, 1597, 1541, 1507, 1467, 1360, 1305, 1213, 1190, 1038, 971. High resolution mass calculated for ($C_{31}H_{31}BF_2N_4O_2$): 540.25081, Found: 540.24910.

## Synthesis of 4

Compound **2** (0.1 mmol, 40 mg) was dissolved in 4 ml solvent (see Table 3), dimedone (0.11 mmol, 15.4 mg) and organocatalyst (0.01 mmol) were added. The mixture was stirred at room temperature for 48 h. The product was purified using flash column chromatography (25% EtOAc/ petroleum ether). 1H NMR (400 MHz, $CDCl_3$): $\delta$ (ppm) = 7.49 (m, 3H, ArH), 7.33 (m, 2H, ArH), 5.98 (s, 1H, CH-pyrrole), 4.51 (s, 2H, $NH_2$), 4.43 (s, 1H, CH), 2.56 (s, 6H, $CH_3$), 2.40 (AB pattern, 2H, $\Delta\delta AB$ =0.06 ppm, J = 16 Hz, $CH_2$), 2.23 (AB pattern, 2H, $\Delta\delta AB$ =0.03 ppm, J = 16 Hz, $CH_2$), 1.58 (s, 6H, $CH_3$), 1.11 (s, 3H, $CH_3$), 1.08 (s, 3H, $CH_3$). 13C NMR (100 MHz, $CDCl_3$): 195.75, 161.08, 157.14, 155.14, 143.04, 135.07, 131.48, 129.89, 128.94, 128.08, 121.09, 118.23, 112.19, 61.20, 50.54, 47.04, 40.41, 31.99, 28.40, 28.00, 25.61, 14.47, 12.48, 11.39, 8.62. IR: $\nu$ ($cm^{-1}$): 3338, 3175, 2957, 2925, 2191, 1680, 166s4, 1598, 1537, 1512, 1465, 1358, 1309, 1191, 1158, 976. Mass calculated for ($C_{31}H_{31}BF_2N_4O_2$) + $CH_3CN$ + Na: 604.26713, Found: 604.26829.

*Monitoring the Michael Reaction*
*between BODIPY-Dicyanoalkene (Compound 1*
*or Compound 2) and Dimedone in the Presence*
*of the Catalysts*

In these reactions, (0.02 mmol) BODIPY-Dicyanoalkene was dissolved in 4 ml 1,2-dichloroethane. The solution was circulated through a 3 mm path length quartz flow cuvette. The emission spectrum of the solution was measured. Then, dimedone (0.03 mmol) and catalyst (0.002 mmol) were added. The emission spectra of the solution were automatically measured every 30 min. The excitation wavelength was $\lambda_{ex}$ = 478 nm.

# References

1. Yeap G-Y, Hrishikesan E, Chan Y-H, Mahmood WAK (2016) A new emissive Chalcone-based chemosensor armed by Coumarin and Naphthol with fluorescence "turn-on" properties for selective detection of F− ions. J Fluoresc. doi:10.1007/s10895-016-1938-5

2. Krumova K, Greene LE, Cosa G (2013) Fluorogenic α-tocopherol analogue for monitoring the antioxidant status within the inner mitochondrial membrane of live cells. J Am Chem Soc 135:17135–17143. doi:10.1021/ja408227f

3. Kofoed J, Darbre T, Reymond JL (2006) Dual mechanism of zinc-proline catalyzed aldol reactions in water. Chem Commun 1482–1484. doi:10.1039/B600703A

4. Uno SN, Tiwari DK, Kamiya M, Arai Y, Nagai T, Urano Y (2015) A guide to use photocontrollable fluorescent proteins and synthetic smart fluorophores for nanoscopy. Microscopy 64:263–277. doi:10.1093/jmicro/dfv037

5. Matsumoto T, Urano Y, Shoda T, Kojima H, Nagano T (2007) A thiol-reactive fluorescence probe based on donor-excited photoinduced electron transfer: key role of Ortho substitution. Org Lett 9:3375–3377. doi:10.1021/ol071352e

6. Matsumoto T, Urano Y, Takahashi Y, Mori Y, Terai T, Nagano T (2011) In situ evaluation of kinetic resolution catalysts for nitroaldol by rationally designed fluorescence probe. J Organomet Chem 76:3616–3625. doi:10.1021/jo1020344

7. Qin W, Vozza A, Brouwer AM (2009) Photophysical properties of cinchona organocatalysts in organic solvents. J Phys Chem C 113:11790–11795. doi:10.1021/jp901867h

8. Qian J, Brouwer AM (2010) Excited state proton transfer in the cinchona alkaloid cupreidine. Phys Chem Chem Phys 12:12562–12569. doi:10.1039/c003419c

9. Kumpulainen T, Brouwer AM (2012) Excited-state proton transfer and ion pair formation in a cinchona organocatalyst. Phys Chem Chem Phys 14:13019–13026. doi:10.1039/c2cp41483j

10. Cordes T, Blum SA (2013) Opportunities and challenges in single-molecule and single-particle fluorescence microscopy for mechanistic studies of chemical reactions. Nat Chem 5:993–999. doi:10.1038/nchem.1800

11. Rybina A, Lang C, Wirtz M, Grußmayer K, Kurz A, Maier F, Schmitt A, Trapp O, Jung G, Herten D-P (2013) Distinguishing alternative reaction pathways by single-molecule fluorescence spectroscopy. Angew Chem Int Ed 52:6322–6325. doi:10.1002/anie.201300100View

12. Rybina A, Thaler B, Krämer R, Herten D-P (2014) Monitoring hydroquinone–quinone redox cycling by single molecule fluorescence spectroscopy. Phys Chem Chem Phys 16:19550–19555. doi:10.1039/C4CP02640C

13. Yue Y, Guo Y, Xu J, Shao S (2011) A Bodipy-based derivative for selective fluorescence sensing of homocysteine and cysteine. New J Chem 35:61–64. doi:10.1039/c0nj00720j

14. Mukai K, Okabe K, Hosose H (1989) Synthesis and stopped-flow investigation of antioxidant activity of tocopherols: finding of new tocopherol derivatives having the highest antioxidant activity among phenolic antioxidants. J Organomet Chem 54:557–560. doi:10.1021/jo00264a011

15. Nour AMM, Khalid SA, Kaiser M, Brun R, Abdalla WE, Schmidt TJ (2010) The antiprotozoal activity of methylated flavonoids from *Ageratum conyzoides* L. J Ethnopharmacol 129:127–130. doi:10.1016/j.jep.2010.02.015

16. He F, Mu L, Yan GL, Liang NN, Pan QH, Wang J, Reeves MJ, Duan CQ (2010) Biosynthesis of anthocyanins and their regulation in colored grapes. Molecules 15:9057–9091. doi:10.3390/molecules15129057

17. Sagar Vijay Kumar P, Suresh L, Vinodkumar T, Reddy BM, Chandramouli GVP (2016) Zirconium doped ceria nanoparticles: an efficient and reusable catalyst for a green multicomponent synthesis of novel Phenyldiazenyl–chromene derivatives using aqueous medium. ACS Sustain Chem Eng 4:2376–2386. doi:10.1021/acssuschemeng.6b00056

18. Stachulski AV, Berry NG, Low LAC, Moores SL, Row E, Warhurst DC, Adagu IS, Rossignol JF (2006) Identification of isoflavone derivatives as effective anticryptosporidial agents in vitro and in vivo. J Med Chem 49:1450–1454. doi:10.1021/jm050973f

19. Poupaert J, Carato P, Colacino E (2005) 2(3H)-Benzoxazolone and bioisosters as "Privileged Scaffold" in the design of pharmacological probes. 2:877–885. doi:10.2174/0929867053507388

20. Dadiboyena S, Nefzi A (2012) Parallel synthesis of structurally diverse aminobenzimidazole tethered sultams and benzothiazepinones. Tetrahedron Lett 53:6897–6900. doi:10.1016/j.tetlet.2012.09.135

21. Evdokimov NM, Kireev AS, Yakovenko AA, Antipin MY, Magedov IV, Kornienko A (2006) Convenient one-step synthesis of a medicinally relevant benzopyranopyridine system. Tetrahedron Lett 47:9309–9312. doi:10.1016/j.tetlet.2006.10.110

22. Yue Y, Yin C, Huo F, Chao J, Zhang Y (2016) Thiol-chromene click chemistry: a turn-on fluorescent probe for specific detection of cysteine and its application in bioimaging. Sensors Actuators B Chem 223:496–500. doi:10.1016/j.snb.2015.09.127

23. Wu B, Gao X, Yan Z, Chen MW, Zhou YG (2015) C-H oxidation/Michael addition/cyclization Cascade for enantioselective synthesis of functionalized 2-amino-4H-chromenes. Org Lett 17:6134–6137. doi:10.1021/acs.orglett.5b03148

24. Osyanin VA, Osipov DV, Klimochkin YN (2012) Convenient one-step synthesis of 4-unsubstituted 2-amino-4H-chromene-2-carbonitriles and 5-unsubstituted 5H-chromeno[2,3-b]pyridine-3-carbonitriles from quaternary ammonium salts. Tetrahedron 68:5612–5618. doi:10.1016/j.tet.2012.04.065

25. Yu N, Aramini JM, Germann MW, Huang Z (2000) Reactions of salicylaldehydes with alkyl cyanoacetates on the surface of solid

catalysts: syntheses of 4H-chromene derivatives. Tetrahedron Lett 41:6993–6996. doi:10.1016/S0040-4039(00)01195-3

26. Kemnitzer W, Kasibhatla S, Jiang S, Zhang H, Zhao J, Jia S, Xu L, Crogan-Grundy C, Denis R, Barriault N, Vaillancourt L, Charron S, Dodd J, Attardo G, Labrecque D, Lamothe S, Gourdeau H, Tseng B, Drewe J, Cai SX (2005) Discovery of 4-aryl-4H-chromenes as a new series of apoptosis inducers using a cell- and caspase-based high-throughput screening assay. 2. Structure-activity relationships of the 7- and 5-, 6-, 8-positions. Bioorg Med Chem Lett 15:4745–4751. doi:10.1016/j.bmcl.2005.07.066

27. Kasibhatla S, Gourdeau H, Meerovitch K, Drewe J, Reddy S, Qiu L, Zhang H, Bergeron F, Bouffard D, Yang Q, Herich J, Lamothe S, Cai SX, Tseng B (2004) Discovery and mechanism of action of a novel series of apoptosis inducers with potential vascular targeting activity. Mol Cancer Ther 3:1365–1374

28. Huang C, Jia T, Tang M, Yin Q, Zhu W, Zhang C, Yang Y, Jia N, Xu Y, Qian X (2014) Selective and ratiometric fluorescent trapping and quantification of protein vicinal dithiols and in situ dynamic tracing in living cells. J Am Chem Soc 136:14237–14244. doi:10.1021/ja5079656

29. Sletten EM, Swager TM (2015) Fluorofluorophores: fluorescent Fluorous chemical tools spanning the visible Spectrum. J Am Chem Soc 16:16333–16339. doi:10.1021/ja507848f

30. Blum SA (2014) Location change method for imaging chemical reactivity and catalysis with single-molecule and particle fluorescence microscopy. Phys Chem Chem Phys 16:16333–16339. doi:10.1039/c4cp00353e

31. Suzuki T, Matsuzaki T, Hagiwara H, Aoki T, Takata K (2007) Recent advances in fluorescent labeling techniques for fluorescence microscopy. Acta Histochem Cytochem 40:131–137. doi:10.1267/ahc.07023

32. Thumser AE, Storch J (2007) Characterization of a BODIPY-labeled fluorescent fatty acid analogue. Binding to fatty acid-binding proteins, intracellular localization, and metabolism. Mol Cell Biochem 299:67–73. doi:10.1007/s11010-005-9041-2

33. Hensle EM, Esfandiari NM, Lim SG, Blum SA (2014) Bodipy fluorophore toolkit for probing chemical reactivity and for tagging reactive functional groups. Eur J Org Chem 16:3347–3354. doi:10.1002/ejoc.201400052

34. Vu TT, Méallet-Renault R, Clavier G, Trofimov BA, Kuimova MK (2016) Tuning BODIPY molecular rotors into the red: sensitivity to viscosity: vs. temperature. J Mater Chem C 4:2828–2833. doi:10.1039/c5tc02954f

35. Yang C, Gong D, Wang X, Iqbal A, Deng M, Guo Y, Tang X, Liu W, Qin W (2016) A new highly copper-selective fluorescence enhancement chemosensor based on BODIPY excitable with visible light and its imaging in living cells. Sensors Actuators B Chem 224:110–117. doi:10.1016/j.snb.2015.10.037

36. Jiao L, Yu C, Li J, Wang Z, Wu M, Hao E (2009) β-formyl-BODIPYs from the Vilsmeier-Haack reaction. J Organomet Chem 74:7525–7528. doi:10.1021/jo901407h

37. Lee CH, Yoon HJ, Shim JS, Jang WD (2012) A boradiazaindacene-based turn-on fluorescent probe for cyanide detection in aqueous media. Chem Eur J 18:4513–4516. doi:10.1002/chem.201200008

38. Jiao L, Liu M, Zhang M, Yu C, Wang Z, Hao E (2011) Visual and colorimetric detection of cyanide anion based on a "turn-off" daylight fluorescent molecule. Chem Lett 40:623–625. doi:10.1246/cl.2011.623

39. Lincoln R, Greene LE, Krumova K, Ding Z, Cosa G (2014) Electronic excited state redox properties for BODIPY dyes predicted from Hammett constants: estimating the driving force of photo-induced electron transfer. J Phys Chem A 118:10622–10630. doi:10.1021/jp5059148

40. Loudet A, Burgess K (2007) BODIPY dyes and their derivatives: syntheses and spectroscopic properties. Chem Rev 107:4891–4932. doi:10.1021/cr078381n

41. Zhang Y, Wang W (2012) Recent advances in organocatalytic asymmetric Michael reactions. Catal Sci Technol 2:42–53. doi:10.1039/C1CY00334H

42. Rueping M, Nachtsheim BJ, Koenigs RM, Ieawsuwan W (2010) Synthesis and structural aspects of N-Triflylphosphoramides and their calcium salts—highly acidic and effective Brønsted acids. Chem Eur J 16:13116–13126. doi:10.1002/chem.201001438

43. Brouwer AM (2011) Standards for photoluminescence quantum yield measurements in solution (IUPAC technical report). Pure Appl Chem 83:2213–2228. doi:10.1351/PAC-REP-10-09-31

44. Würth C, Grabolle M, Pauli J, Spieles M, Resch-Genger U (2013) Relative and absolute determination of fluorescence quantum yields of transparent samples. Net Protoc 8:1535–1550. doi:10.1038/nprot.2013.087

45. Magde D, Wong R, Seybold PG (2002) Fluorescence quantum yields and their relation to lifetimes of rhodamine 6G and fluorescein in nine solvents: improved absolute standards for quantum yields. Photochem Photobiol 75:327–334. doi:10.1562/0031-8655(2002)0750327FQYATR2.0.CO2

46. Kaik M, Gawroński J (2003) Facile monoprotection of trans-1,2-diaminocyclohexane. Tetrahedron Asymmetry 14:1559–1563. doi:10.1016/S0957-4166(03)00308-2

47. Puglisi A, Benaglia M, Annunziata R, Siegel JS (2012) Immobilization of chiral bifunctional organocatalysts on poly(methylhydrosiloxane). ChemCatChem 4:972–975. doi:10.1002/cctc.201200114

48. Breman AC, Telderman SEM, Van Santen RPM, Scott JI, Van Maarseveen JH, Ingemann S, Hiemstra H (2015) Cinchona alkaloid catalyzed sulfa-Michael addition reactions leading to Enantiopure β-functionalized cysteines. J Organomet Chem 80:10561–10574. doi:10.1021/acs.joc.5b01660

49. Rurack K, Spieles M (2011) Fluorescence quantum yields of a series of red and near-infrared dyes emitting at 600-1000 nm. Anal Chem 83:1232–1242. doi:10.1021/ac101329h